

Research Article

Dynamical Analysis of Posttreatment HIV-1 Infection Model

M. Pradeesh ¹, A. Manivannan ², S. Lakshmanan ², F. A. Rihan ³, and Prakash Mani ¹

¹Division of Mathematics, School of Advanced Sciences, Vellore Institute of Technology, Vellore, India

²Division of Mathematics, School of Advanced Sciences, Vellore Institute of Technology, Chennai, India

³Department of Mathematical Sciences, Faculty of Science, UAE University, Al-Ain, UAE

Correspondence should be addressed to Prakash Mani; prakashgru88@gmail.com

Received 30 May 2022; Revised 29 July 2022; Accepted 8 August 2022; Published 8 October 2022

Academic Editor: Abdellatif Ben Makhlof

Copyright © 2022 M. Pradeesh et al. This is an open access article distributed under the Creative Commons Attribution License, which permits unrestricted use, distribution, and reproduction in any medium, provided the original work is properly cited.

This paper aims to explore the dynamic characteristics of the post treatment human immunodeficiency virus (HIV) type-1 model by proposing the theoretical frameworks. Distinct from the previous works, this study explores the effect of effector cells, loss of functional effector cells, and two types of anti-retroviral therapies such as reverse transcriptase inhibitors (RTIs) and protease inhibitors (PIs) and also the effect of intracellular time delay. Based on the Routh—Hurwitz criterion and eigenvalue analysis, the stability of the proposed HIV-1 model is analyzed. To reveal the significance of time delay, the Hopf-type bifurcation analysis is performed. The optimal control algorithm is designed by choosing the antiviral therapies such as RTI and PI as control parameters. Numerical simulations are performed to validate the effectiveness of the proposed theoretical frameworks.

1. Introduction

According to the World Health Organization (WHO), 680,000 individuals died from HIV-1-related diseases worldwide in 2020, ranging from 480,000 to 1.0 million, while 1.5 million people were newly infected with HIV-1. Antiretroviral therapy (ART) has drastically reduced the number of people infected with HIV during the 1990s, with 27.5 million (approximately) people undergoing treatment in 2020. Because of antiretroviral medication, the HIV infection rate has decreased by 49% over the last two decades, from 2000 to 2020. Despite the researcher's valiant efforts in terms of treatment options and drugs, a cure for HIV-1 remains a pipe dream, necessitating lifelong treatment. Mathematical models have been demonstrated to be a useful tool for comprehending the dynamics of disease progression, identifying key determinants, and evaluating the efficacy of antiretroviral therapy.

During the 1990s, HIV was thought to be a lethal disease, similar to other lentiviruses, because HIV remains within the host without causing symptoms and progresses to a chronic stage known as acquired immunodeficiency

virus (AIDS), with a nearly ten-year delay between HIV and AIDS. In this case, mathematical modeling of HIV can help in estimating the lifespan of infected cells, evaluating therapeutic efficacy, and realizing that new virions require a host with deoxyribonucleic acid (DNA) to replicate. Currently, a variety of therapy options are available to help people with HIV get better. However, controlling the virus is the only option available and curing the disease still requires seamless efforts in the research domain.

Mathematical models have been created to investigate the dynamic properties of cell populations using parameters including latent reservoirs, immunological responses, total carrying capacity, and time-delayed fractional differential operators based on literature reviews (see [1–5]). Immature infected cells also known as latent stage are those that have been infected but are not yet infectious, which is considered in the present study. Immune responses such as CD4+ T-cells/CD8+ T-cells are activated when a foreign agent enters the body, causing the body's alarm system to go into overdrive [6, 7].

When systems are in motion, there will always be a degree of lag time. Time delays are inevitable because it has

an ability to cause a significant impact on cell populations. When modeling the kinetics of HIV-1 infection, two types of delays are taken into account. One situation is that the uninfected cells interact with infected/free virions and there is an intracellular temporal delay. Besides, after a foreign agent has been ingested, immune response cells must be activated, which results in a delay in the immunological response. This study aims to explore the effect of intracellular time delay with respect to infected cell population [8, 9]. Initially, ART is given to every primarily infected HIV person, but based on the stage of infection the level of drugs may be redefined. However, it is a challenging task with respect to the immune boosters which may vary in the individual. Besides, it can be seen that, if there is a change in the period of drugs provided, then it will reflect in the virion populations. Hence, this study explores the effect of antiretroviral therapies which are suggested as posttreatment for a long period of time. The proposed model's stability analysis will provide some insights into disease progression in relation to the system parameters such as infection rate and time delays. Followed by, bifurcation analysis is used to determine the threshold value of the significant parameter that has the potential to cause fluctuations in the cell population. The optimal control algorithm is designed by selecting cell populations, which aids in better understanding and extraction of system parameters, resulting in cell populations with stable staining [10–13]. Recently, the models were proposed on Zika virus, HIV, SARS-CoV-2, and other viral dynamics models such as maize streak virus in maize spread by leaf hopper mostly in Africa, canine distemper virus, and rabies epidemics in red fox with respect to significant factors such as vaccination parameter involved models and optimal control strategies (for more details, refer [14–22]). Distinct from the existing models, the present study focuses on considering the effect of time delays and two kinds of antiretroviral therapies. The overall contribution is listed in the following:

- (1) This paper models the dynamics of HIV-1 infection by considering the factors such as healthy CD4+ cells, latent reservoirs, infected cells, free virions, and immune responses also considering the effect of time delay.
- (2) Positivity and boundedness of solutions of the differential model are proved. The reproduction number is determined through the next-generation matrix, which helps to identify the community spread.
- (3) Conditions for the existence of Hopf bifurcation are proved by choosing the intracellular time delay as a bifurcation parameter.
- (4) Optimal control algorithm is designed to ensure the stabilization of the proposed model.
- (5) Numerical simulations are performed to validate the proposed theoretical frameworks.

2. Model of Posttreatment HIV-1 Viral Dynamics

The schematic representation of our model is given below.

$$\begin{aligned}
 \dot{x}(t) &= s - \gamma x(t) - (1 - \varepsilon_1(t))\beta x(t)y(t - \tau), \\
 \dot{l}(t) &= \alpha_L(1 - \varepsilon_1(t))\beta x(t)y(t) + (\rho - a - d_L)l(t), \\
 \dot{y}(t) &= (1 - \alpha_L)(1 - \varepsilon_1(t))\beta x(t)y(t) + al(t) \\
 &\quad - \delta y(t) - my(t)z(t), \\
 \dot{u}(t) &= (1 - \varepsilon_2(t))py(t) - cu(t), \\
 \dot{z}(t) &= b_z \frac{y(t)}{K_B + y(t)} z(t) - d_z \frac{(t)}{K_D + y(t)} z(t) - \mu z(t).
 \end{aligned} \tag{1}$$

In model (1), the first equation represents the rate of change in the susceptible cell populations, where s denotes the rate of production, γ is decay rate and $\varepsilon_1, \varepsilon_2$ denotes the efficacy of antiretroviral therapies. Consider that $\varepsilon_i(t)$, where $i = 1, 2$, in $[0, 1]$; if $\varepsilon_i = 1$, where $i = 1, 2$, then cent percent the treatment is effective which makes the infection zero, and if $\varepsilon_i(t) = 0$, $i = 1, 2$, then, no progress in the therapy. β represents the rate of infection between the infected and uninfected cell population. τ stands for intracellular time delay. The second equation describes the state of latent infection; that is, target cells are infected but not yet infectious. Suppose if the infected cells are matured enough to infect the susceptible cells. ρ, α_L , and d_L are scalars. The third equation explains the rate of change in the infectious cell population with the death rate δ , migrated from latent infection a , removing the infection by immune responses at the rate of m . The fourth equation explores the rate of change in the free virions; the rate of proliferation from the infection is given by p and the decay rate is c . Finally, the production of effector cells can have the maximum proliferation in an infected cell with a maximum rate b_z and is given by the term $b_z (y(t)/y(t) + K_B)z(t)$. The loss of functional effector cells is defined by $d_z (y(t)/y(t) + K_D)z(t)$, with an assumption $K_D > K_B$.

2.1. Positivity and Boundedness. In order to ensure the convergence of the solutions of the model, it becomes necessary to ensure that solutions of the state variables in model (1) are positive and ultimately bounded.

Theorem 1. *Assume that $(x(t), l(t), y(t), u(t), z(t))$ be a solution of the proposed model (1) with the initial conditions $x(t) > 0, l(t) > 0, y(t) > 0, u(t) > 0, z(t) > 0$. It is positive and ultimately bounded for $t > 0$.*

Proof. Consider the proof regarding $x(t) > 0$ for all $t > 0$. In this regard, assume that there exists $t_1 > 0$, which implies $x(t_1) = 0, x(t) > 0, t \in [0, t_1)$ such that $\dot{x}(t) \leq 0$. From (1), it is clear that $\dot{x}(t_1) = s, s > 0$, which is a contradiction and leads to the proof that $x(t) > 0, \forall t > 0$.

Similarly, the proof can be extended for all the remaining state equations.

$$\begin{aligned}
l(t) &= l(0)e^{-(a+d_L-\rho)t} + \int_0^t \alpha_L(1-\epsilon_1(t))\beta x(\xi)y(\xi)e^{(a+d_L-\rho)(\xi-t)}d\xi, \\
z(t) &= z(0)e^{\int_0^t (b_z y(\xi)/K_B + y(\xi)z(\xi) - d_z y(\xi)/K_D + y(\xi)z(\xi) - \mu)d\xi}, \\
y(t) &= y(0)e^{-\delta t} + \int_0^t ((1-\alpha_L)(1-\epsilon_1(t))\beta x(\xi)y(\xi) + al(\xi) \\
&\quad - my(\xi)z(\xi))e^{-\delta(\xi-t)}d\xi, \\
u(t) &= u(0)e^{-ct} + \int_0^t (1-\epsilon_2(t))ye^{c(\xi-t)}d\xi.
\end{aligned} \tag{2}$$

Now, to prove $\{l(t), y(t), u(t), z(t)\} > 0, \forall t > 0$. And consider that $t_2 > 0$ and define

$$\min\{l(t_2), y(t_2), u(t_2), z(t_2)\} = 0. \tag{3}$$

If $l(t_2) = 0, l(t) > 0$ for $t \in [0, t_2)$ and $y(t) > 0, u(t) > 0, z(t) > 0$ for $t \in [0, t_2), \dot{l}(t_2) = 0$, then we have $\dot{l}(t_2) = \alpha_L(1-\epsilon_1(t_2))\beta x(t_2)y(t_2) > 0$, which is a contradiction.

If $y(t_2) = 0, y(t) > 0$ for $t \in [0, t_2)$ and $\{l(t), u(t), z(t)\} > 0$ for $t \in [0, t_2)$ with $\dot{y}(t_2) \leq 0$. However, from (1), one can have $\dot{y}(t_2) = al(t_2) > 0$.

Similarly, for $u(t_2) = 0$ and $z(t_2) = 0$ is also a contradiction. Thus, $\{x(t), l(t), y(t), u(t), z(t)\} > 0, \forall t > 0$. To proceed with ensuring the boundedness of the solutions, we extend the results of the positivity of the solution for model (1).

$$\dot{x}(t) \leq s - \gamma x(t). \tag{4}$$

Taking the limits will lead to

$$\limsup_{t \rightarrow \infty} (x(t)) \leq \frac{s}{\gamma}. \tag{5}$$

Let $H(t) = x(t) + l(t) + y(t)$

$$\dot{H}(t) = \dot{x}(t) + \dot{l}(t) + \dot{y}(t)$$

$$\begin{aligned}
\dot{H}(t) &= s - \gamma x(t) - (1-\epsilon_1(t))\beta x(t)y(t) \\
&\quad + \alpha_L(1-\epsilon_1(t))\beta x(t)y(t) + (\rho - a - d_L)l(t) \\
&\quad + (1-\alpha_L)(1-\epsilon_1(t))\beta x(t)y(t) \\
&\quad + al(t) - \delta y(t) - my(t)z(t) \\
&\leq s - \gamma x(t) + (\rho - d_L)l(t) - \delta y(t) \\
&\leq s + \sigma H(t).
\end{aligned} \tag{6}$$

Define that $\sigma = \min\{\gamma, (\rho - d_L), \delta\}$ and

$$\limsup_{t \rightarrow \infty} (H(t)) \leq \frac{s}{\sigma}. \tag{7}$$

To prove the ultimate boundedness of free virions, the same approach is followed:

$$\dot{u}(t) = py(t) - cu(t) = p\left(\frac{s}{\sigma}(1-\epsilon_2(t))\right) - cu(t) \tag{8}$$

$$\lim_{t \rightarrow \infty} \sup (u(t)) \leq \frac{ps(1-\epsilon_2(t))}{\sigma c}.$$

Since $u(t)$ cannot be negative, if $\epsilon_2(t) = 0$, then $\sup(u(t)) = 0$. Similarly, for $z(t)$, we get

$$\begin{aligned}
\dot{z}(t) &= b_z \frac{y(t)}{K_B + y(t)} z(t) - d_z \frac{y(t)}{K_D + y(t)} z(t) - \mu z(t), \\
\frac{\dot{z}(t)}{z} &= b_z \frac{y(t)}{K_B + y(t)} - d_z \frac{y(t)}{K_D + y(t)} - \mu.
\end{aligned} \tag{9}$$

Applying integration on both sides

$$\limsup_{t \rightarrow \infty} (z(t)) \leq b_z \Omega_1 - d_z \Omega_2 - \mu, \tag{10}$$

where

$$\begin{aligned}
\Omega_1 &= b_z \frac{(s/\sigma)}{K_B + (s/\sigma)}, \\
\Omega_2 &= d_z \frac{(s/\sigma)}{K_D + (s/\sigma)}.
\end{aligned} \tag{11}$$

Hence, it is proved that all the state variables solutions are ultimately bounded.

Consider

$$\begin{aligned}
\Delta &= \left\{ (x, l, y, u, z) \in C_+^5: \|x(t)\| \leq \frac{s}{\sigma} \|l(t)\| \right. \\
&\leq \frac{s}{\sigma} \|y(t)\| \leq \frac{s}{\sigma} \|u(t)\| \leq \frac{ps(1-\epsilon_2(t))}{\sigma c}
\end{aligned} \tag{12}$$

$$\|z(t)\| \leq b_z \Omega_1 - d_z \Omega_2 - \mu,$$

where σ, Ω_1 , and Ω_2 are given in the above equation. From the given theorem, it is clear that, within the region, Δ is a positive invariant. \square

3. Equilibria

This section describes the derivation of equilibria of PTC HIV model based on three cases such as disease-free, immune-free equilibrium, and endemic equilibrium.

(i) Model (1) without infection exhibits disease-free equilibrium $E_0 = (x_0, 0, 0, 0, 0)$, where $x_0 = s/d$.

(ii) If $R_0 > 1$, model (1) has an immune-free equilibrium $E_1 = (x_1, l_1, y_1, u_1, 0)$ with the coefficients

$$\begin{aligned}
x_1 &= \frac{\delta(a + d_L - \rho)}{\beta(1-\epsilon_1(t))[a\alpha_L + (1-\alpha_L)(a + d_L - \rho)]}, \\
l_1 &= \frac{\alpha_L \beta (1-\epsilon_1(t)) x_1 y_1}{a + d_L - \rho},
\end{aligned} \tag{13}$$

$$u_1 = \frac{p(1-\epsilon_2(t))_1}{c},$$

$$y_1 = \frac{d(R_0 - 1)}{\beta(1-\epsilon_1(t))}.$$

(iii) The endemic equilibrium of the system $E_2(x_+, l_+, y_+, u_+, z_+)$ is given by

$$\begin{aligned}
x_+ &= \frac{s}{\gamma + \beta(1 - \epsilon_1(t))y_+}, \\
l_+ &= \frac{\alpha_L(1 - \epsilon_1(t))\beta x_+ y_+}{a + d_L - \rho} \\
y_+ &= \frac{-(K_y) + \sqrt{(K_y)^2 - 4(I)(C)}}{2I}, \\
u_+ &= p_+ \left(\frac{1 - \epsilon_2(t)}{c, z_+ = \frac{(a + d_L - \rho)(1 - \alpha_L)(1 - \epsilon_1(t))\beta x_+ + a\alpha_L(1 - \epsilon_1(t))\beta x_+ y_+ - \delta(a + d_L - \rho)}{m(a + d_L - \rho)}} \right),
\end{aligned} \tag{14}$$

with $K_y = K_D b_z - d_z K_B - \mu K_B - \mu K_D$ and $I = b_z - d_z - \mu$, $C = -\mu K_B K_D$.

3.1. Basic Reproduction Number. In epidemiology, a basic reproduction number is the average number of persons an affected person can transmit the secondary infection. The basic reproduction number is an indicator that helps to determine the community spread of infection, which can be calculated using the next generation matrix. For the proposed model, the basic reproduction number, say, R_0 , is determined for various situations and described in the following sections.

3.1.1. For Disease-Free Equilibrium. The basic reproduction number of the model without a viral latent reservoir is

$$\begin{aligned}
(1 - \epsilon_1(t))\beta x(t)y(t) - \delta y(t) &> 0, \\
((1 - \epsilon_1(t))\beta x(t) - \delta)y(t) &> 0.
\end{aligned} \tag{15}$$

Since $y(t) \neq 0$, then

$$R_0 = (1 - \epsilon_1(t))\beta \cdot \frac{s}{\gamma} \cdot \frac{1}{\delta}. \tag{16}$$

3.1.2. For Immune-Free Equilibrium. The basic reproduction number of the model with immune-free equilibrium is

$$\begin{aligned}
\mathcal{F} &= \begin{pmatrix} \alpha_L(1 - \epsilon_1(t))\beta x(t)y(t) \\ (1 - \alpha_L)(1 - \epsilon_1(t))\beta x(t)y(t) \end{pmatrix}, \\
\mathcal{V} &= \begin{pmatrix} (\rho - a - d_L)l(t) \\ al(t) - \delta y(t) \end{pmatrix}.
\end{aligned} \tag{17}$$

Then, \mathcal{F} and \mathcal{V} help us to find the next generation matrix FV^{-1} as calculated:

$$\begin{aligned}
F &= \begin{pmatrix} 0 & \alpha_L(1 - \epsilon_1(t))\beta x(t) \\ 0 & (1 - \alpha_L)(1 - \epsilon_1(t))\beta x(t) \end{pmatrix}, \\
V &= \begin{pmatrix} \rho - a - d_L & 0 \\ a & -\delta \end{pmatrix}, \\
V^{-1} &= \frac{1}{-\delta(\rho - a - d_L)} \begin{pmatrix} -\delta & 0 \\ -a & \rho - a - d_L \end{pmatrix}, \\
FV^{-1} &= \begin{pmatrix} 0 & \alpha_L(1 - \epsilon_1(t))\beta x(t) \\ 0 & (1 - \alpha_L)(1 - \epsilon_1(t))\beta x(t) \end{pmatrix} \cdot \frac{1}{-\delta(\rho - a - d_L)} \begin{pmatrix} -\delta & 0 \\ -a & \rho - a - d_L \end{pmatrix}, \\
&= \begin{pmatrix} \frac{-a\alpha_L(1 - \epsilon_1(t))\beta x(t)}{\delta(a + d_L - \rho)} & \frac{-\alpha_L(1 - \epsilon_1(t))\beta x(t)}{\delta} \\ \frac{-a(1 - \alpha_L)(1 - \epsilon_1(t))\beta x(t)}{\delta(a + d_L - \rho)} & \frac{-(1 - \epsilon_1(t))(1 - \alpha_L)\beta x(t)}{\delta} \end{pmatrix}.
\end{aligned} \tag{18}$$

Now, the characteristic equation for the above matrix is

$$\lambda^2 - \left[\frac{-a\alpha_L(1-\varepsilon_1(t))\beta x(t)}{\delta(a+d_L-\rho)} - \frac{(1-\varepsilon_1(t))(1-\alpha_L)\beta x(t)}{\delta} \right], \quad (19)$$

$$\lambda + \left(\frac{-\alpha_L(1-\varepsilon_1(t))\beta x(t)}{\delta} \right) \left(\frac{-a(1-\alpha_L)(1-\varepsilon_1(t))\beta x(t)}{\delta(a+d_L-\rho)} \right) = 0,$$

where $x_0 = s/Y$, then the basic reproduction number is given by

$$R_0 = (1 - \varepsilon_1(t)) \cdot \beta \cdot \left[(1 - \alpha_L) + \frac{a\alpha_L}{a + d_L - \rho} \right] \cdot \frac{s}{Y} \cdot \frac{1}{\delta} \quad (20)$$

3.1.3. *For Endemic Equilibrium.* The basic reproduction number of the model with endemic equilibrium is given by

$$\mathcal{F} = \begin{pmatrix} \alpha_L(1 - \varepsilon_1(t))\beta x(t)y(t) \\ (1 - \alpha_L)(1 - \varepsilon_1(t))\beta x(t)y(t) \end{pmatrix}, \quad (21)$$

$$\mathcal{V} = \begin{pmatrix} (\rho - a - d_L)l(t) \\ al(t) - \delta y(t) \end{pmatrix}.$$

Then, \mathcal{F} and \mathcal{V} help us to find the next generation matrix FV^{-1} as calculated below:

$$F = \begin{pmatrix} 0 & \alpha_L(1 - \varepsilon_1(t))\beta x(t) \\ 0 & (1 - \alpha_L)(1 - \varepsilon_1(t))\beta x(t) \end{pmatrix},$$

$$V = \begin{pmatrix} \rho - a - d_L & 0 \\ a & -\delta \end{pmatrix},$$

$$V^{-1} = \frac{1}{-\delta(\rho - a - d_L)} \begin{pmatrix} -\delta & 0 \\ -a & \rho - a - d_L \end{pmatrix}, \quad (22)$$

$$FV^{-1} = \begin{pmatrix} 0 & \alpha_L(1 - \varepsilon_1(t))\beta x(t) \\ 0 & (1 - \alpha_L)(1 - \varepsilon_1(t))\beta x(t) \end{pmatrix} \cdot \frac{1}{-\delta(\rho - a - d_L)} \begin{pmatrix} -\delta & 0 \\ -a & \rho - a - d_L \end{pmatrix},$$

$$= \begin{pmatrix} \frac{-a\alpha_L(1 - \varepsilon_1(t))\beta x(t)}{\delta(a + d_L - \rho)} & \frac{-\alpha_L(1 - \varepsilon_1(t))\beta x(t)}{\delta} \\ \frac{-a(1 - \alpha_L)(1 - \varepsilon_1(t))\beta x(t)}{\delta(a + d_L - \rho)} & \frac{-(1 - \varepsilon_1(t))(1 - \alpha_L)\beta x(t)}{\delta} \end{pmatrix}.$$

Now, the characteristic equation for the above matrix is

$$\lambda^2 - \left[\frac{-a\alpha_L(1 - \varepsilon_1(t))\beta x(t)}{\delta(a + d_L - \rho)} - \frac{(1 - \varepsilon_1(t))(1 - \alpha_L)\beta x(t)}{\delta} \right],$$

$$\lambda + \left(\frac{-\alpha_L(1 - \varepsilon_1(t))\beta x(t)}{\delta} \right) \left(\frac{-a(1 - \alpha_L)(1 - \varepsilon_1(t))\beta x(t)}{\delta(a + d_L - \rho)} \right) = 0. \quad (23)$$

The basic reproduction number is calculated from the next generation matrix is given by

$$\lambda = \frac{2Is\beta(1 - \varepsilon_1(t))[a\alpha_L + (a + d_L - \rho)(1 - \alpha_L)]}{\delta(a + d_L - \rho) \left\{ 2I\gamma + \beta(1 - \varepsilon_1(t)) \left[-(K_y + \sqrt{(K_y)^2 - 4IC}) \right] \right\}}, \quad (24)$$

where K_y , I , and C are described above. The spectral radius or the largest eigenvalue of the next generation matrix is called the basic reproduction number.

4. Stability Analysis

Let $E_2(x_+, l_+, y_+, u_+, z_+)$ be any arbitrary positive equilibrium of the system (1). Then, the Jacobian matrix was

evaluated at positive equilibrium's E_2 in the view of biological aspects. This leads us to the following characteristic

$$J = \begin{pmatrix} -\gamma - (1 - \varepsilon_1(t))\beta y & 0 & -(1 - \varepsilon_1(t))\beta x e^{-\lambda\tau} & 0 & 0 \\ \alpha_L(1 - \varepsilon_1(t))\beta y & \rho - a - d_L & \alpha_L(1 - \varepsilon_1(t))\beta x & 0 & 0 \\ \beta y(1 - \alpha_L)(1 - \varepsilon_1(t)) & a & a_{33} & 0 & -my \\ 0 & 0 & p(1 - \varepsilon_2(t)) & -c & 0 \\ 0 & 0 & a_{53} & 0 & a_{55} \end{pmatrix}, \quad (25)$$

where $a_{33} = \beta x(1 - \alpha_L)(1 - \varepsilon_1(t)) - mz - \delta$, $a_{53} = (b_z z / K_B + y) - (d_z z / K_D + y) - (b_z y z / (K_B + y)^2) + (d_z y z / (K_D + y)^2)$ and $a_{55} = (b_z y / K_B + y) - \mu - (d_z y / K_D + y)$

4.1. Stability Analysis of the Model without Time Delay. The characteristic polynomial without delay is given by

$$\lambda^5 + P_1\lambda^4 + P_2\lambda^3 + P_3\lambda^2 + P_4\lambda + P_5 = 0. \quad (26)$$

Routh–Hurwitz criterion: define n^{th} root-based Routh–Hurwitz matrix as follows:

$$H_n = \begin{pmatrix} P_1 & 1 & 0 & 0 & \cdots & 0 \\ P_3 & P_2 & P_1 & 1 & \cdots & 0 \\ P_5 & P_4 & P_3 & P_2 & \cdots & 1 \\ \vdots & \vdots & \vdots & & & \\ 0 & 0 & 0 & 0 & \cdots & P_n \end{pmatrix}, \quad (27)$$

where $P_j = 0$, if $j > n$. When $n = 5$, the matrix is simplified into

$$H_5 = \begin{pmatrix} P_1 & 1 & 0 & 0 & 0 \\ P_3 & P_2 & P_1 & 1 & 0 \\ P_5 & P_4 & P_3 & P_2 & 1 \\ 0 & 0 & P_5 & P_4 & P_3 \\ 0 & 0 & 0 & 0 & P_5 \end{pmatrix}. \quad (28)$$

Suppose all the roots of the characteristic polynomial with negative real part, then the determinant of Routh–Hurwitz matrices are positive and vice versa. That is, $\det H_i > 0, i = 1, 2, \dots, 5$. This can be employed to verify the proof of Theorem 1. The necessary and sufficient condition to exist for the negative real part for equation (6) is $P_1 > 0, P_1 P_2 - P_3 > 0, P_1(P_2 P_3 - P_1 P_4) + (P_3^2 - P_1 P_5) > 0, P_1[P_2(P_3 P_4 - P_2 P_5) - P_1(P_4^2 + P_4 P_5)] - [P_3(P_3 P_4 - P_2 P_5) + P_1(P_4 P_5) + P_5^2] > 0$, and $\det(H_5) > 0$.

The expansion of the coefficients P_1, P_2, P_3, P_4, P_5 is given in Appendix.

4.2. Stability Analysis of the Model with Time Delay. The characteristic polynomial of the Jacobian is

polynomial. The plus signs are ignored for the convenience of calculations.

$$\lambda^5 + Q_1\lambda^4 + Q_2\lambda^3 + Q_3\lambda^2 + Q_4\lambda + Q_5 + e^{-\lambda\tau}(R_1\lambda^3 + R_2\lambda^2 + R_3\lambda + R_4) = 0. \quad (29)$$

The coefficients $Q_i, i = 1, 2, 3, 4, 5$, and $R_i, i = 1, 2, 3, 4$, are given in Appendix. We rewrite the above equation as

$$Q(\lambda) + e^{-\lambda\tau}R(\lambda) = 0. \quad (30)$$

Suppose some of the eigenvalues are purely imaginary, that is, $\lambda = i\omega$, then the characteristic equation becomes

$$\begin{aligned} & (i\omega)^5 + Q_1(i\omega)^4 + Q_2(i\omega)^3 + Q_3(i\omega)^2 + Q_4(i\omega) \\ & + Q_5 + e^{-i\omega\tau}(R_1(i\omega)^3 + R_2(i\omega)^2 + R_3(i\omega) + R_4) = 0, \\ & i\omega^5 + Q_1\omega^4 - iQ_2\omega^3 - Q_3\omega^2 + iQ_4\omega + Q_5 \\ & + e^{-i\omega\tau}(-R_1i\omega^3 - R_2\omega^2 + iR_3\omega + R_4) = 0, \\ & i(\omega^5 - Q_2\omega^3 + Q_4\omega) + (Q_1\omega^4 - Q_3\omega^2 + Q_5) \\ & + (\cos \omega\tau - i \sin \omega\tau)(-iR_1\omega^3 - R_2\omega^2 + iR_3\omega + R_4) = 0, \\ & i(\omega^5 - Q_2\omega^3 + Q_4\omega) + (Q_1\omega^4 - Q_3\omega^2 + Q_5) \\ & + (\cos \omega\tau - i \sin \omega\tau)(i(-R_1\omega^3 + R_3\omega) - R_2\omega^2 + R_4) = 0. \end{aligned} \quad (31)$$

Equating real and imaginary parts in the above equation:

$$\begin{aligned} & \omega^5 - Q_2\omega^3 + Q_4\omega + \cos \omega\tau(-R_1\omega^3 - R_3\omega) \\ & - i \sin \omega\tau(-R_2\omega^2 + R_4) = 0, \end{aligned} \quad (32)$$

$$\begin{aligned} & Q_1\omega^4 - Q_3\omega^2 + Q_5 + \cos \omega\tau(-R_2\omega^2 + R_4) \\ & + i \sin \omega\tau(-R_1\omega^3 + R_3\omega) = 0. \end{aligned} \quad (33)$$

Squaring and adding equations (32) and (33), we get

$$\begin{aligned}
& (\omega^5 - Q_2\omega^3 + Q_4\omega)^2 + (Q_1\omega^4 - Q_3\omega^2 + Q_5)^2 \\
&= \cos^2\omega\tau(-R_2\omega^2 + R_4)^2 + \sin^2\omega\tau(-R_1\omega^3 + R_3\omega)^2 \\
&\quad + \cos^2\omega\tau(-R_1\omega^3 + R_3\omega)^2 + \sin^2\omega\tau(-R_2\omega^2 + R_4)^2, \quad (34) \\
& (\omega^5 - Q_2\omega^3 + Q_4\omega)^2 + (Q_1\omega^4 - Q_3\omega^2 + Q_5)^2 \\
&= (-R_1\omega^3 + R_3\omega)^2 + (-R_2\omega^2 + R_4)^2.
\end{aligned}$$

Simplifying the above equations leads to the following:
 $-\omega^{10} + (-Q_1^2 + 2Q_2)\omega^8 + (-Q_3^2 + R_1^2 - 2Q_4 + 2Q_1Q_3)\omega^6 + (-Q_5^2 + R_2^2 - 2Q_1Q_5 + 2Q_2Q_4 - 2R_1R_3)\omega^4 + (-Q_4^2 + R_3^2 + 2Q_3Q_5 - 2R_2R_4)\omega^2 - Q_5^2 + R_4^2 = 0.$

Since this is the differential equation of order 10, we get almost "10" roots such as $\omega_1 = z_1, \omega_2 = z_2, \omega_3 = z_3, \omega_4 = z_4, \omega_5 = z_5, \omega_6 = z_6, \omega_7 = z_7, \omega_8 = z_8, \omega_9 = z_9,$ and $\omega_{10} = z_{10}.$

Eliminating $\cos\omega\tau$ from equations (32) and (33), we get

$$\begin{aligned}
\sin\omega\tau &= \frac{(\omega^5 - Q_2\omega^3 + Q_4\omega)A - (Q_1\omega^4 - Q_3\omega^2 + Q_5)B}{A^2 + B^2}, \\
\omega\tau &= \sin^{-1}\left(\frac{(\omega^5 - Q_2\omega^3 + Q_4\omega)A - (Q_1\omega^4 - Q_3\omega^2 + Q_5)B}{A^2 + B^2}\right), \quad (35) \\
\tau^i &= \frac{1}{\omega}\sin^{-1}\left(\frac{(\omega^5 - Q_2\omega^3 + Q_4\omega)A - (Q_1\omega^4 - Q_3\omega^2 + Q_5)B}{A^2 + B^2}\right),
\end{aligned}$$

where $i = 0, 1, 2, \dots,$ $A = (R_4 - R_2\omega^2)$ and $B = (-R_1\omega^3 + R_3\omega).$

Hence, for $\tau = 0,$ E_2 is asymptotically stable by Routh-Hurwitz criterion [1], E_2 remains stable for $\tau < \tau^0;$ we choose

$$\tau^0 = \min(\tau^j), \quad (36)$$

which completes the proof.

5. Hopf Bifurcation Analysis

In general, any physical system will reflect the changes in the qualitative behavior subject to states and parameters changes; for instance, changes in the rate of infection will reflect in the cell populations. Hence, determining the significant parameters that have an ability to affect the stability of the systems is considered bifurcation parameters. By choosing bifurcation parameters, various kinds of solution nature can be realized; among that Hopf-type bifurcation explores the point where solution trajectories cross the origin, say, from negative to positive, in which the system has purely imaginary eigenvalues. The present model possesses the Hopf-type bifurcation while the bifurcation parameter exceeds the threshold value. The process of deriving the stability conditions and proving the existence of Hopf bifurcation are given below.

Theorem 2. Consider that the characteristic polynomial is of the form

$$f_0(\lambda) + f_1(\lambda)e^{-\lambda\tau} = 0, \quad (37)$$

where f_0 and f_1 are continuously differentiable with respect to $\lambda.$ One of the roots is $\lambda(\tau) = \alpha(\tau) + i\omega(\tau),$ where $\lambda(\tau)$ is continuously differentiable with respect to $\tau,$ and satisfies $\alpha(\tau_0) = 0$ and $\omega(\tau_0) = \omega_0$ for a positive real number $t_0.$ Denote

$$\phi(\omega) = |f_0(i\omega)|^2 - |f_1(i\omega)|^2, \quad (38)$$

which results in

$$\text{sign}\left[\frac{d\text{Re}(\lambda)}{d\tau}\bigg|_{\tau=\tau_0}\right] = \text{sign}\left[\left(\frac{1}{2\omega}\frac{d\phi}{d\omega}\right)\bigg|_{\omega=\omega_0}\right]. \quad (39)$$

Proof. Consider equation (38), and by taking the derivative of $|f_0(i\omega)|^2$ with respect to $\omega,$ will lead to

$$\begin{aligned}
\frac{d}{d\omega}(|f_0(i\omega)|^2) &= \frac{d}{d\omega}\{[\text{Re}f_0(i\omega)]^2 + [\text{Im}f_0(i\omega)]^2\} \\
&= 2\text{Re}f_0(i\omega).\text{Re}[f_0'(i\omega)i] + 2\text{Im}f_0(i\omega).\text{Im}[f_0'(i\omega)i] \quad (40) \\
&= 2\text{Re}[\overline{f_0(i\omega)}f_0'(i\omega)i] \\
&= -2\text{Im}[\overline{f_0(i\omega)}f_0'(i\omega)].
\end{aligned}$$

Then,

$$\begin{aligned}
\frac{1}{2\omega}\frac{d\phi}{d\omega} &= \frac{d}{d\omega}(|f_0(i\omega)|^2 - |f_1(i\omega)|^2) \\
&= \frac{1}{\omega}\text{Im}[\overline{f_1(i\omega)}f_1'(i\omega) - \overline{f_0(i\omega)}f_0'(i\omega)] \quad (41) \\
&= \text{Im}\left[|f_1(i\omega)|^2\frac{f_1'(i\omega)}{\omega f_1(i\omega)} - |f_0(i\omega)|^2\frac{f_0'(i\omega)}{\omega f_0(i\omega)}\right].
\end{aligned}$$

Since $|f_0(i\omega_0)|^2 = |f_1(i\omega_0)|^2,$ we have

$$\left(\frac{1}{2\omega}\frac{d\phi}{d\omega}\right)\bigg|_{\omega=\omega_0} = |f_0(i\omega_0)|^2\text{Im}\left[\frac{f_1'(i\omega_0)}{\omega_0 f_1(i\omega_0)} - \frac{f_0'(i\omega_0)}{\omega_0 f_0(i\omega_0)}\right]. \quad (42)$$

Now, we turn to the left side of (38), calculating the derivative of both sides of $f_0(\lambda) + f_1e^{-\lambda\tau} = 0$ with respect to $\tau,$ we obtain

$$f_0'(\lambda) \frac{d\lambda}{d\tau} + f_1'(\lambda) \frac{d\lambda}{d\tau} e^{-\lambda\tau} - \left(\lambda + \tau \frac{d\lambda}{d\tau} f_1(\lambda) e^{-\lambda\tau} \right) = 0. \quad (43)$$

Thus,

$$\begin{aligned} \left[\frac{d\lambda}{d\tau} \right]^{-1} &= \frac{f_0'(\lambda) + f_1(\lambda) e^{-\lambda\tau} - \tau f_1(\lambda) e^{-\lambda\tau}}{\lambda f_1(\lambda) e^{-\lambda\tau}} \\ &= \frac{f_0'(\lambda) e^{\lambda\tau} + f_1'(\lambda)}{\lambda f_1(\lambda)} - \frac{\tau}{\lambda}. \end{aligned} \quad (44)$$

Since $f_0(i\omega_0) + f_1(i\omega_0)e^{-i\omega_0\tau_0} = 0$, we have

$$\begin{aligned} \operatorname{Re} \left[\frac{d\lambda}{d\tau} \Big|_{\tau=\tau_0} \right]^{-1} &= \operatorname{Re} \left[\frac{f_0'(i\omega_0) e^{i\omega_0\tau_0} + f_1'(i\omega_0)}{\omega_0 f_1(i\omega_0)} \right] \\ &= \operatorname{Re} \left[\frac{f_0'(i\omega_0)}{\omega_0 f_0(i\omega_0)} i \right] + \operatorname{Re} \left[\frac{f_1'(i\omega_0)}{\omega_0 f_1(i\omega_0)} i \right] \\ &= \operatorname{Im} \left[\frac{f_1'(i\omega_0)}{\omega_0 f_1(i\omega_0)} - \frac{f_0'(i\omega_0)}{\omega_0 f_0(i\omega_0)} \right]. \end{aligned} \quad (45)$$

Therefore,

$$\begin{aligned} \operatorname{sign} \left[\frac{d\operatorname{Re}(\lambda)}{d\tau} \Big|_{\tau=\tau_0} \right] &= \operatorname{sign} \operatorname{Re} \left[\frac{d\lambda}{d\tau} \Big|_{\tau=\tau_0} \right] \\ &= \operatorname{sign} \operatorname{Re} \left[\frac{d\lambda}{d\tau} \Big|_{\tau=\tau_0} \right]^{-1} \\ &= \operatorname{sign} \left[\left(\frac{1}{2\omega} \frac{d\phi}{d\omega} \right) \Big|_{\omega=\omega_0} \right]. \end{aligned} \quad (46)$$

The proof is completed. \square

6. Optimal Control Design

Considering (1), based on two variables such as RTI and PI as controls, namely, ε_1 and ε_2 . Here, ε_1 represents the drug reverse transcriptase, and it safeguards the healthy CD4+ from infection, so that the healthy immune cells are maintained in the right proportion. Also, ε_2 is represented the drug protease inhibitors, which maintains the release of the free virions to burst which are active and fully infected. In general, the treatment is initiated with an antiretroviral drug or the combination of two or more drugs, which creates some side effects while using a regular basis. Since the decision of choosing the drug combination is complex and, in this regard, an optimal strategy is a useful tool to understand the situation and make decisions. Now, optimal control provides different options with respect to estimating the costs of the drugs used for the therapies and observing the drug's effectiveness for the disease. The therapy should last long as the optimal control helps us to find the suitable drug combination for the disease. Formulating the optimization problem based on optimal pair, existence is discussed in the following sections.

6.1. The Optimization Problem. In order to state the optimization problem, we first consider ε_1 and ε_2 vary with time.

$$\dot{x}(t) = s - \gamma x(t) - (1 - \varepsilon_1(t))\beta x(t)y(t),$$

$$\dot{l}(t) = \alpha_L(1 - \varepsilon_1(t))\beta x(t)y(t) + (\rho - a - d_L)l(t),$$

$$\begin{aligned} \dot{y}(t) &= (1 - \alpha_L)(1 - \varepsilon_1(t))\beta x(t)y(t) \\ &\quad + al(t) - \delta y(t) - my(t)z(t), \end{aligned} \quad (47)$$

$$\dot{u}(t) = p(1 - \varepsilon_2(t))y(t) - cu(t),$$

$$\dot{z}(t) = b_z \frac{y(t)}{K_B + y(t)} z(t) - d_z \frac{y(t)}{K_D + y(t)} z(t) - \mu z(t).$$

The optimization problem is designed in terms of maximizing the following objective function constructed from the model parameters:

$$J(\varepsilon_1, \varepsilon_2) = \int_0^{t_f} x(t) + z(t) + u(t) - \left[\frac{A_1}{2} \varepsilon_1^2(t) + \frac{A_2}{2} \varepsilon_2^2(t) \right] dt. \quad (48)$$

Here, the upper bound t_f denotes the period of the treatment and assumptions $A_1 > 0$ and $A_2 > 0$, respectively, stand for benefit and treatment costs. The scalars $\varepsilon_1(t)$ and $\varepsilon_2(t)$ are bounded and Lebesgue integrable. The objective of the control is to increase the uninfected cell populations through immune cells and decrease the cell count of free virions and infected cells. Hence, $(\varepsilon_1^*, \varepsilon_2^*)$ is the control pair that needs to be investigated. We assume that the control pair is nonempty, convex, and closed and it is integrable in the objective functional.

$$J(\varepsilon_1^*, \varepsilon_2^*) = \max \{ J(\varepsilon_1, \varepsilon_2) : (\varepsilon_1, \varepsilon_2) \in U \}, \quad (49)$$

where U is the control set defined by $U = \{ \varepsilon_1(t), \varepsilon_2(t) : \varepsilon_i(t) \text{ measurable, } 0 \leq \varepsilon_i \leq 1, t \in [0, t_f], i = 1, 2 \}$.

6.2. Optimal System. In order to investigate the properties of the optimal system, the Pontryagin's minimum principle given in [13] is utilized and it provides necessary stability conditions for the designed optimal control problem. The advantage of the principle is that it handles (47)–(49) in terms of maximizing a Hamiltonian H through ε_1 and ε_2

$$\begin{aligned} H(t, x, l, y, u, z, \gamma, \varepsilon_1, \varepsilon_2, \lambda) \\ = \frac{A_1}{2} \varepsilon_1^2 + \frac{A_2}{2} \varepsilon_2^2 - x - u - z + \sum_{i=0}^5 \lambda_i f_i, \end{aligned} \quad (50)$$

with

$$\begin{aligned} f_1 &= s - \gamma x - (1 - \varepsilon_1)\beta x y \tau \\ f_2 &= \alpha_L(1 - \varepsilon_1)\beta x y + (\rho - a - d_L)l, \\ f_3 &= (1 - \alpha_L)(1 - \varepsilon_1)\beta x y + al - \delta y - myz, \\ f_4 &= p(1 - \varepsilon_2)y - cu, \end{aligned} \quad (51)$$

$$f_5 = b_z \frac{y}{K_B + y} z - d_z \frac{y}{K_D + y} z - \mu z.$$

Based on the above discussion, the following theorem can be derived.

Theorem 3. For any optimal control ε_1^* , ε_2^* , and solutions x^* , l^* , y^* , u^* , z^* of the corresponding state system (1), there exists adjoint variables λ_1 , λ_2 , λ_3 , λ_4 , and λ_5 satisfying the equations

$$\begin{aligned}
\lambda_1'(t) &= 1 + \lambda_1(t)(Y + \beta(1 - \varepsilon_1(t + \tau))y(t)) + \lambda_2(t)(\alpha_L(\varepsilon_1 - 1)\beta y(t)) + \lambda_3(t)(1 - \alpha_L)(\varepsilon_1 - 1)\beta y(t) \\
\lambda_2'(t) &= \lambda_2(t)(-\rho + a + d_L) - \lambda_3(t)(a), \\
\lambda_3'(t) &= \lambda_1(t)\beta x(t)[1 - (\varepsilon_1(t + \tau))] + \lambda_2(t)[\alpha_L(\varepsilon_1(t) - 1)\beta x(t)], \\
&\quad + \lambda_3(t)[(1 - \alpha_L)(\varepsilon_1(t) - 1)\beta x(t) + \delta + mz(t)] + \lambda_4(t)\rho(\varepsilon_2(t) - 1), \\
&\quad + \lambda_5(t)\left[-\frac{b_z z(t)}{k_B + y(t)} + \frac{d_z z(t)}{k_D + y(t)} + \frac{b_z y(t)z(t)}{(k_B + y(t))^2} - \frac{d_z y(t)z(t)}{(k_D + y(t))^2}\right], \\
\lambda_4'(t) &= 1 + c\lambda_4(t), \\
\lambda_5'(t) &= 1 + \lambda_3(t)(my(t)) + \lambda_5(t)\left[d_z \frac{y(t)}{K_D + y(t)} - b_z \frac{y(t)}{K_B + y(t)} + \mu\right],
\end{aligned} \tag{52}$$

with the transversality conditions

$$\lambda_i(t_f) = 0, i = 1, \dots, 5. \tag{53}$$

Moreover, the optimal control is given by

$$\begin{aligned}
\varepsilon_1^* &= \min\left(1, \max\left(0, -\frac{\beta}{A_1}[\lambda_1 x^*(t)y_{\tau}^*]\right)\right), \\
\varepsilon_2^* &= \min\left(1, \max\left(0, \frac{\rho}{A_2}[\lambda_4 y^*(t)]\right)\right).
\end{aligned} \tag{54}$$

Proof. The adjoint equations and transversality conditions can be obtained by using Pontryagin's minimum principle with delay, such that suppose if consider the equation in the vector for $X = (\lambda_1, \lambda_2, \lambda_3, \lambda_4, \lambda_5)$.

$$\begin{aligned}
\lambda_1'(t) &= -\left(\frac{\partial(\dot{x}(t))}{\partial x(t)} \quad \frac{\partial(\dot{l}(t))}{\partial x(t)} \quad \frac{\partial(\dot{y}(t))}{\partial x(t)} \quad \frac{\partial(\dot{u}(t))}{\partial x(t)} \quad \frac{\partial(\dot{z}(t))}{\partial x(t)}\right)X^T - \frac{\partial H}{\partial x}, \\
\lambda_2'(t) &= -\left(\frac{\partial(\dot{x}(t))}{\partial l(t)} \quad \frac{\partial(\dot{l}(t))}{\partial l(t)} \quad \frac{\partial(\dot{y}(t))}{\partial l(t)} \quad \frac{\partial(\dot{u}(t))}{\partial l(t)} \quad \frac{\partial(\dot{z}(t))}{\partial l(t)}\right)X^T - \frac{\partial H}{\partial l}, \\
\lambda_3'(t) &= -\left(\frac{\partial(\dot{x}(t))}{\partial y(t)} \quad \frac{\partial(\dot{l}(t))}{\partial y(t)} \quad \frac{\partial(\dot{y}(t))}{\partial y(t)} \quad \frac{\partial(\dot{u}(t))}{\partial y(t)} \quad \frac{\partial(\dot{z}(t))}{\partial y(t)}\right)X^T - \frac{\partial H}{\partial y}, \\
\lambda_4'(t) &= -\left(\frac{\partial(\dot{x}(t))}{\partial u(t)} \quad \frac{\partial(\dot{l}(t))}{\partial u(t)} \quad \frac{\partial(\dot{y}(t))}{\partial u(t)} \quad \frac{\partial(\dot{u}(t))}{\partial u(t)} \quad \frac{\partial(\dot{z}(t))}{\partial u(t)}\right)X^T - \frac{\partial H}{\partial u}, \\
\lambda_5'(t) &= -\left(\frac{\partial(\dot{x}(t))}{\partial z(t)} \quad \frac{\partial(\dot{l}(t))}{\partial z(t)} \quad \frac{\partial(\dot{y}(t))}{\partial z(t)} \quad \frac{\partial(\dot{u}(t))}{\partial z(t)} \quad \frac{\partial(\dot{z}(t))}{\partial z(t)}\right)X^T - \frac{\partial H}{\partial z}.
\end{aligned} \tag{55}$$

The optimal control ε_1^* and ε_2^* can be solved from the optimality conditions

$$\frac{\partial H}{\partial \varepsilon_1}(t) = 0, \frac{\partial H}{\partial \varepsilon_2}(t) = 0. \tag{56}$$

That is,

$$\begin{aligned} \frac{\partial H}{\partial \varepsilon_1}(t) &= A_1 \varepsilon_1 + \beta(x(t)y_\tau)\lambda_1 = 0, \\ \frac{\partial H}{\partial \varepsilon_2}(t) &= A_2 \varepsilon_2 - \lambda_4 p y(t) = 0. \end{aligned} \quad (57)$$

Consider the optimal controls ε_1^* and ε_2^* defined in (54) are bounded. If we substitute ε_1^* and ε_2^* in systems (47) and (52), we obtain the following optimality system:

$$\begin{aligned} \dot{x}^*(t) &= s - \Upsilon x^*(t) - (1 - \varepsilon_1^*(t))\beta x^*(t)y^*(t - \Gamma), \\ \dot{l}^*(t) &= \alpha_L(1 - \varepsilon_1^*(t))\beta x^*(t)y^*(t) + (\rho - a - d_L)l^*(t), \\ \dot{y}^*(t) &= (1 - \alpha_L)(1 - \varepsilon_1^*(t))\beta x^*(t)y^*(t) + al^*(t) - \delta y^*(t) - my^*(t)z^*(t), \\ \dot{u}^*(t) &= p(1 - \varepsilon_2^*(t))y^*(t) - cu^*(t), \\ \dot{z}^*(t) &= b_z \frac{y^*(t)}{K_B + y^*(t)} z^*(t) - d_z \frac{y^*(t)}{K_D + y^*(t)} z^*(t) - \mu z^*(t), \\ \lambda'_1(t) &= 1 + \lambda_1(t)(\Upsilon + \beta(1 - \varepsilon_1(t + \tau))y(t)) + \lambda_2(t)(\alpha_L(\varepsilon_1 - 1)\beta y(t)) \\ &\quad + \lambda_3(t)(1 - \alpha_L)(\varepsilon_1 - 1)\beta y(t), \\ \lambda'_2(t) &= \lambda_2(t)(-\rho + a + d_L) - \lambda_3(t)(a), \\ \lambda'_3(t) &= \lambda_1(t)\beta x(t)[1 - (\varepsilon_1(t + \tau))] + \lambda_2(t)[\alpha_L(\varepsilon_1(t) - 1)\beta x(t)] \\ &\quad + \lambda_3(t)[(1 - \alpha_L)(\varepsilon_1(t) - 1)\beta x(t) + \delta + mz(t)] + \lambda_4(t)\rho(\varepsilon_2(t) - 1) \\ &\quad + \lambda_5(t) \left[\frac{b_z z(t)}{k_B + y(t)} + \frac{d_z z(t)}{k_D + y(t)} + \frac{b_z y(t)z(t)}{(k_B + y(t))^2} - \frac{d_z y(t)z(t)}{(k_D + y(t))^2} \right], \\ \lambda'_4(t) &= 1 + c\lambda_4(t), \\ \lambda'_5(t) &= 1 + \lambda_3(t)(my(t)) + \lambda_5(t) \left[d_z \frac{y(t)}{K_D + y(t)} - b_z \frac{y(t)}{K_B + y(t)} + \mu \right], \\ \varepsilon_1^* &= \min \left(1, \max \left(0, -\frac{\beta}{A_1} [\lambda_1 x^*(t)y_\tau^*] \right) \right), \\ \varepsilon_2^* &= \min \left(1, \max \left(0, \frac{p}{A_2} [\lambda_4 y^*(t)] \right) \right), \\ \lambda_i(t_f) &= 0, \quad i = 1, \dots, 5. \end{aligned} \quad (58)$$

The significance of stability conditions, validating the existence of Hopf bifurcation properties, and effect of the optimal controller are explored in the following section. \square

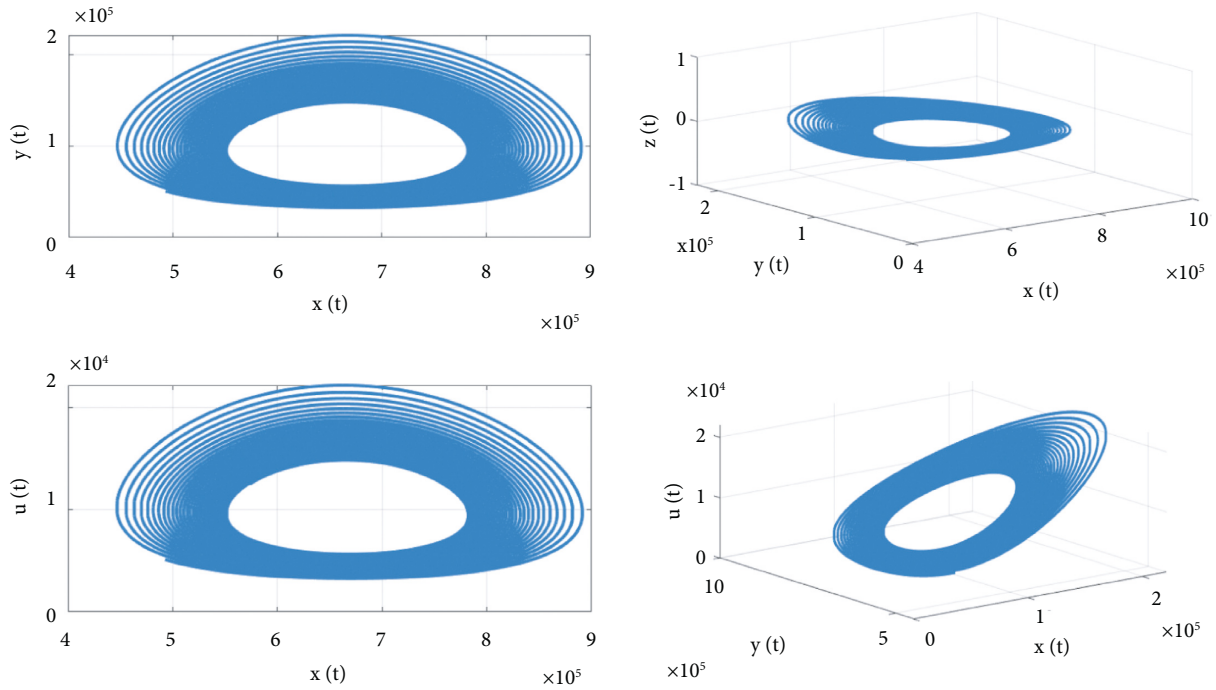
7. Numerical Simulation

This section describes the numerical evaluations of the proposed model (1) by choosing the experimental range of parameter values provided in Table 1. The simulations are performed through Runge–Kutta fourth-order numerical approximation scheme. The outcomes of the cell simulations

corresponding to cell populations are demonstrated through phase-space diagrams. Figures 1 and 2 illustrate the solution behavior of cell populations within the threshold and exceeding the threshold of time delay, respectively. Also, Figure 3 explores the effect of optimal control design, in which the objective is achieved by increasing the number of uninfected cell populations and diminishing the number of virions. In addition, Figures 4–7 provide insights by comparing the controlled and uncontrolled system states such as uninfected, infected, latent, and free virions, respectively. Figure 2 shows the interpretation of variables of the

TABLE 1: Parameter values and their sources.

| Notations | Values | References |
|------------|-------------------------------|------------|
| s | 10^5 cells/mL/day | [23] |
| γ | 0.01 | — |
| β | 1.5×10^{-6} (mL/day) | [24, 25] |
| δ | 1 day^{-1} | [26] |
| N | 2000 | [27, 28] |
| p | 2000 day^{-1} | — |
| C | 23 day^{-1} | [29] |
| ϵ | 0.001 | — |
| A | 0.001 day^{-1} | — |
| d_L | 0.004 day^{-1} | [30] |
| $t_{1/2}$ | 44 months | [31] |
| ρ | 0.0045 day^{-1} | [32] |
| α_L | 10^{-6} | — |
| s_z | 1 cells/mL/day | — |
| b_z | 1 day^{-1} | [33] |
| K_B | 0.1 cells/mL | [34] |
| d_z | 2 day^{-1} | [35] |
| K_D | 5 cells/mL | [34] |
| μ | 0.0002 day^{-1} | — |
| M | 0.42 mL/cells/day | — |

FIGURE 1: Unstable responses for the time delay $\tau > 0.93$.

equilibrium when $\tau < 0.93$. The top left corner in the panel of Figure 2 evidence the rate of change in healthy CD4+ and infected cells and the bottom left depicts the uninfected cells and the free virions. Similarly, the phase portrait of all the cell populations such as uninfected and infected cells with free virions and immune cells is accordingly picturized. The drug parameter $\epsilon_1(t)$ and the transmission rate β have a high influence on the stability of the

equilibrium. That is, for $0 \leq \epsilon_1(t) \leq 0.6$, the equilibrium is stable. For $1.5 \times 10^{-7} \leq \beta \leq 1.5 \times 10^{-6}$, the equilibrium remains stable. When the transmission rate gets higher or lesser, it loses the stability of equilibrium, where α_L , r , μ , and a also affect the stability when it increases rapidly. The rest of the parameters are having less significance in terms of stability when compared with the remaining parameters.

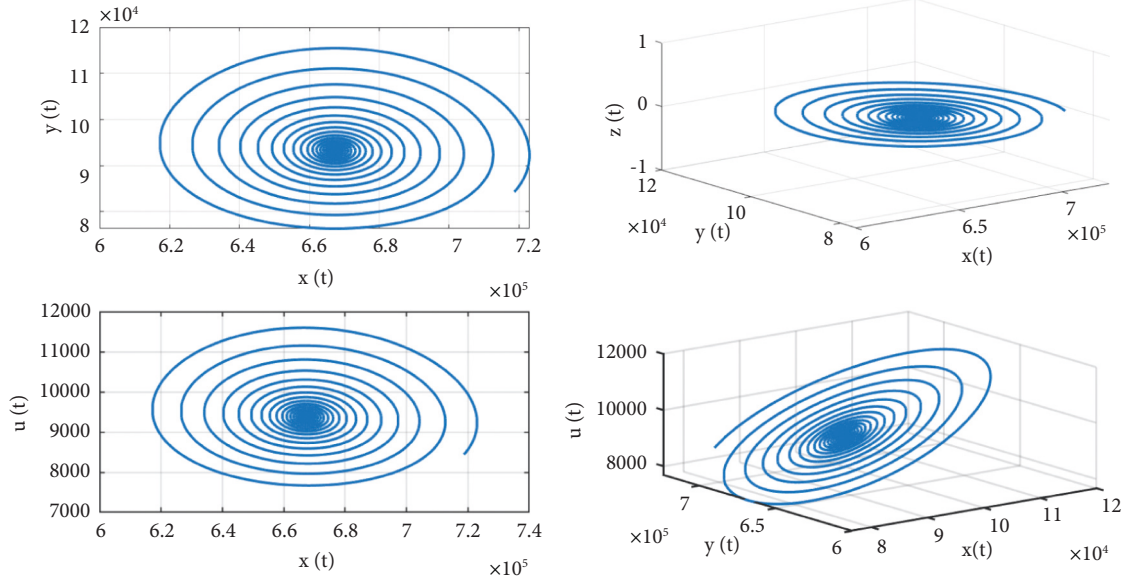


FIGURE 2: Stable responses for the time delay $\tau < 0.93$.

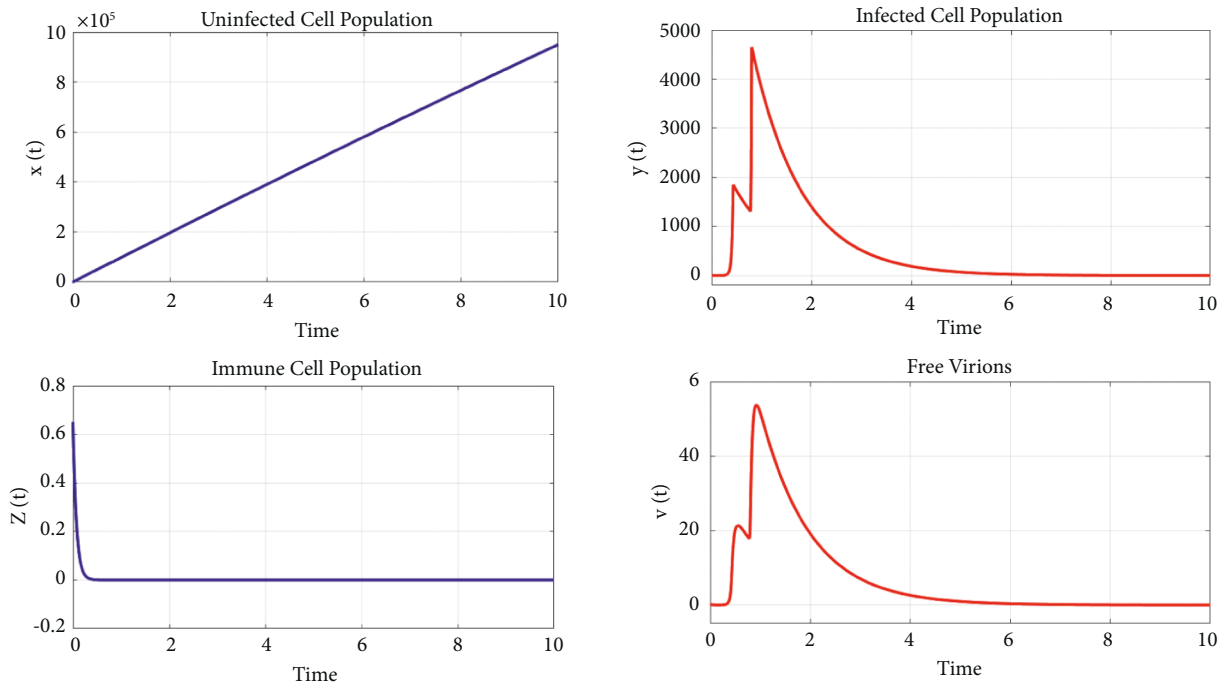


FIGURE 3: Optimal control-based state responses with respect to time.

Figure 1 represents the state trajectories where the equilibrium point loses its stability due to time delay that makes the transmission rate slow. If the drug is already administered into the body, the drug starts to function among the cells; there is a period for the drug to make progress and with respect to time delays, it becomes necessary to have the effect of time response,

and if the drug efficacy is not up to expectation, then the endemic equilibrium will lose the stability.

Figure 8 shows that the uninfected cells start to bifurcate as τ crosses the value 0.93.

Figures 3 represents the uninfected cell population after the optimal control is established. The top figures show the

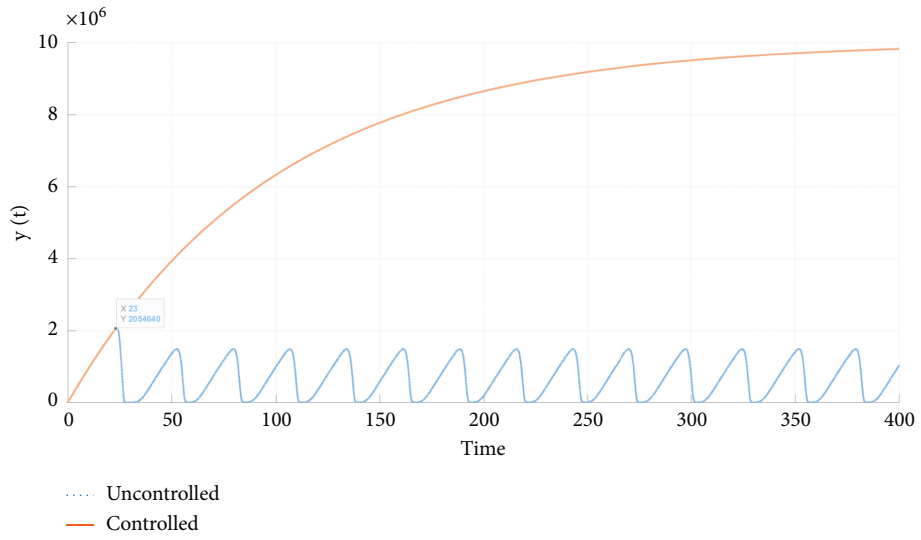


FIGURE 4: Comparison of controlled and uncontrolled susceptible cell populations.

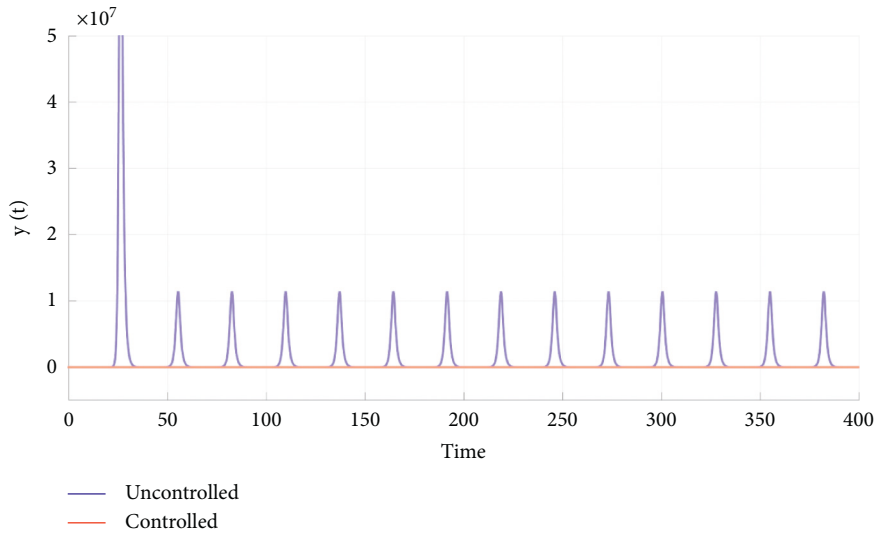


FIGURE 5: Comparison of controlled and uncontrolled infected cell populations.

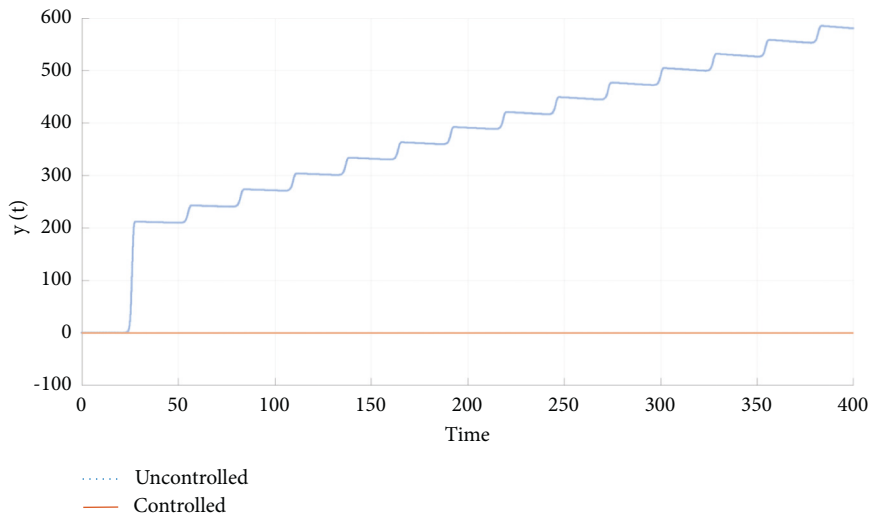


FIGURE 6: Comparison of controlled and uncontrolled latent cell populations.

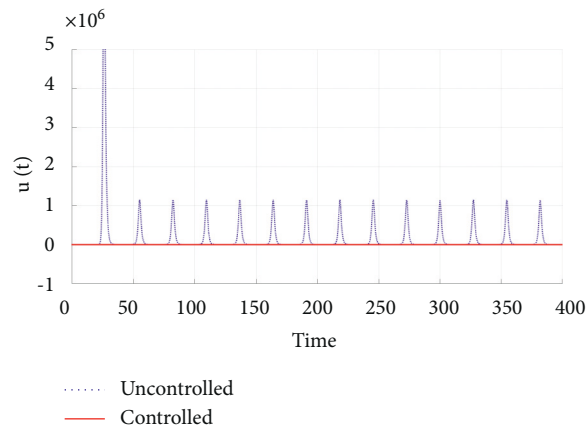


FIGURE 7: Comparison of controlled and uncontrolled free virions.

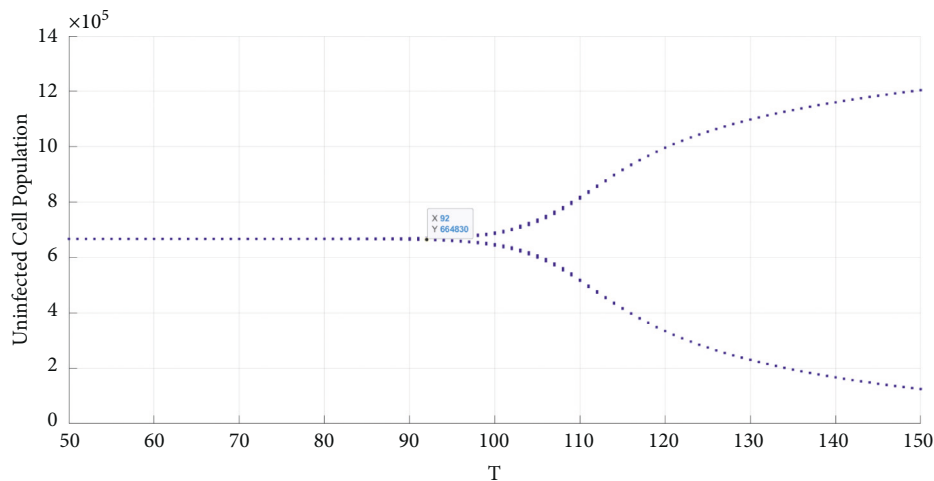


FIGURE 8: Bifurcation behavior for time delay with respect to uninfected cell populations.

increasing cell population of the uninfected cells and the reducing rate of the infected cells; it is visible after a certain stage the immune cells maintained in proportion, with no increasing number of cells. Similarly, the free virions are depleted in the process.

Figures 4–7 provide the comparisons between controlled and uncontrolled susceptible cell populations, infected cell populations, latent cell populations, and free virions. The graphs exhibit the controlled cell population after the implementation of optimal control.

8. Conclusion

The aim of the paper is to explore the dynamical analysis of posttreatment HIV-1 infection with respect to various significant parameters such as the effect of time delays, two different kinds of antiretroviral therapies, and loss of functional effector cells. By employing the Routh–Hurwitz criterion, the stability properties of the model with respect to discrete-type constant time-delay which is chosen as a bifurcation parameter

have been presented. To ensure the effect of time delays, the existence of Hopf-type bifurcation in the behavior of solutions has been proved through proving the corresponding transversality conditions. To reveal the effect of combination of drug therapies, along with those parameters, the situation is modeled as an optimal control problem in terms of the objective function. Through objective function, the results explore the maximization in the number of uninfected cell population and minimization in the number of infected cells and corresponding results are picturized in the numerical section. In the future direction, the model can be extended in terms of fractional order differential operator, considering continuous-type time-delays, stochastic disturbances, and impulse in the antiviral therapy, which also plays a significant role in the system dynamics.

Appendix

The coefficient of system variables is provided in the following:

$$\begin{aligned}
& C_{11} \\
C_{22} &= \rho - a - d_L; C_{23} \\
C_{53} &= \frac{b_z z}{K_B + y} - \frac{d_z z}{K_D + y} - \frac{b_z y z}{(K_B + y)^2} + \frac{b_z y z}{(K_D + y)^2}; C_{55} \\
Q_1 &= (c - C_{22} - C_{33} - C_{55} - C_{11}) \\
Q_2 &= (C_{11}C_{22} - C_{11}c - C_{22}c - C_{33}cC_{23}a + C_{11}C_{33} + C_{22}C_{33} + C_{11}C_{55}C_{22}C_{55}) \\
&\quad + C_{33}C_{55} - C_{35}C_{53} \\
Q_3 &= (C_{11}C_{35}C_{53} - C_{11}C_{22}C_{55} - C_{11}C_{33}C_{55} - C_{11}C_{22}C_{33} - C_{22}C_{33}C_{55} \\
&\quad + C_{22}C_{35}C_{53} + C_{11}C_{23}a + C_{23}C_{55}a + C_{11}C_{22}c + C_{11}C_{33}c + C_{22}C_{33}c \\
&\quad + C_{11}C_{55}c + C_{22}C_{55}c + C_{33}C_{55}c - C_{35}C_{53}c - C_{23}ac) \\
Q_4 &= (C_{11}C_{22}C_{33}C_{55} - C_{11}C_{22}C_{35}C_{53} - C_{11}C_{23}C_{55}a - C_{11}C_{22}C_{33}c \\
&\quad - C_{11}C_{22}C_{55}c - C_{11}C_{33}C_{55}c + C_{11}C_{35}C_{53}c - C_{22}C_{33}C_{55}c \\
&\quad + C_{22}C_{35}C_{53}c + C_{11}C_{23}ac + C_{23}C_{55}ac) \\
Q_5 &= C_{11}C_{22}C_{33}C_{55}c - C_{11}C_{22}C_{35}C_{53}c - C_{11}C_{23}C_{55}ac \\
R_1 &= -C_{13}C_{31} \\
R_2 &= (C_{13}C_{22}C_{31} + C_{13}C_{31}C_{55} - C_{13}C_{21}a - C_{13}C_{31}c), \\
R_3 &= (C_{13}C_{21}C_{55}a - C_{13}C_{22}C_{31}C_{55} + C_{13}C_{22}C_{31}c + C_{13}C_{31}C_{55}c - C_{13}C_{21}ac) \\
R_4 &= -C_{13}C_{22}C_{31}C_{55}c + C_{13}C_{21}C_{55}ac \\
P_1 &= (c - C_{22} - C_{33} - C_{55} - C_{11}), \\
P_2 &= (C_{11}C_{22} - C_{11}c - C_{22}c - C_{33}c - C_{55}c - C_{23}a + C_{11}C_{33} - C_{13}C_{31} \\
&\quad + C_{22}C_{33} + C_{11}C_{55} + C_{22}C_{55} + C_{33}C_{55} - C_{35}C_{53}), \\
P_3 &= (C_{13}C_{22}C_{31} - C_{11}C_{22}C_{33} - C_{11}C_{22}C_{55} - C_{11}C_{33}C_{55} + C_{11}C_{35}C_{53} \\
&\quad + C_{13}C_{31}C_{55} - C_{22}C_{33}C_{55} + C_{22}C_{35}C_{53} + C_{11}C_{23}a \\
&\quad - C_{13}C_{21}a + C_{23}C_{55}a + C_{11}C_{22}c + C_{11}C_{33}c \\
&\quad - C_{13}C_{31}c + C_{22}C_{33}c + C_{11}C_{55}c + C_{22}C_{55}c \\
&\quad + C_{33}C_{55}c - C_{35}C_{53}c - C_{23}ac), \\
P_4 &= (C_{11}C_{22}C_{33}C_{55} - C_{11}C_{22}C_{35}C_{53} - C_{13}C_{22}C_{31}C_{55} - C_{11}C_{23}C_{55}a + C_{13}C_{21}C_{55}a - C_{11}C_{22}C_{33}c \\
&\quad + C_{13}C_{22}C_{31}c - C_{11}C_{22}C_{55}c - C_{11}C_{33}C_{55}c + C_{11}C_{35}C_{53}c + C_{13}C_{31}C_{55}c \\
&\quad - C_{22}C_{33}C_{55}c + C_{22}C_{35}C_{53}c + C_{11}C_{23}ac - C_{13}C_{21}ac + C_{23}C_{55}ac), \\
P_5 &= C_{11}C_{22}C_{33}C_{55}c - C_{11}C_{22}C_{35}C_{53}c - C_{13}C_{22}C_{31}C_{55}c - C_{11}C_{23}C_{55}ac + C_{13}C_{21}C_{55}ac.
\end{aligned} \tag{A.1}$$

Data Availability

All the data are available within the article.

Conflicts of Interest

The authors declare that there are no conflicts of interest.

References

- [1] M. Prakash, R. Rakkiyappan, A. Manivannan, and J. Cao, "Dynamical analysis of antigen-driven t-cell infection model with multiple delays," *Applied Mathematics and Computation*, vol. 354, pp. 266–281, 2019.
- [2] T. Wang, Z. Hu, and F. Liao, "Stability and hopf bifurcation for a virus infection model with delayed humoral immunity response," *Journal of Mathematical Analysis and Applications*, vol. 411, no. 1, pp. 63–74, 2014.
- [3] X. Wang, S. Tang, X. Song, and L. Rong, "Mathematical analysis of an hiv latent infection model including both virus-to-cell infection and cell-to-cell transmission," *Journal of Biological Dynamics*, vol. 11, no. sup2, pp. 455–483, 2017.
- [4] T. K. Ayele, E. F. Doungmo Goufo, and S. Mugisha, "Mathematical modeling of hiv/aids with optimal control: a case study in Ethiopia," *Results in Physics*, vol. 26, Article ID 104263, 2021.
- [5] A. M. Elaiw, N. H. AlShamrani, and A. D. Hobiny, "Mathematical modeling of hiv/htlv co-infection with ctl-mediated immunity," *AIMS Mathematics*, vol. 6, no. 2, pp. 1634–1676, 2021.
- [6] Z. Liu, L. Wang, and R. Tan, "Spatiotemporal dynamics for a diffusive hiv-1 infection model with distributed delays and ctl immune response," *Discrete & Continuous Dynamical Systems-B*, vol. 27, no. 5, p. 2767, 2022.
- [7] L. Noël, R. Tubiana, A. Simon et al., "Low immune response rate of hiv-infected patients to a single injection of hepatitis a vaccine," *Infectious Disease News*, vol. 51, no. 1, pp. 94–96, 2021.
- [8] N. H. AlShamrani, "Stability of an htlv-hiv coinfection model with multiple delays and ctl-mediated immunity," *Advances in Difference Equations*, vol. 2021, no. 1, pp. 270–357, 2021.
- [9] H. Liu and J.-F. Zhang, "Dynamics of two time delays differential equation model to hiv latent infection," *Physica A: Statistical Mechanics and Its Applications*, vol. 514, pp. 384–395, 2019.
- [10] H.-D. Kwon, J. Lee, and S.-D. Yang, "Optimal control of an age-structured model of hiv infection," *Applied Mathematics and Computation*, vol. 219, no. 5, pp. 2766–2779, 2012.
- [11] J. Danane and K. Allali, "Optimal control of an HIV model with CTL cells and latently infected cells," *Numerical Algebra, Control and Optimization*, vol. 10, no. 2, pp. 207–225, 2020.
- [12] G. Akudibillah, A. Pandey, and J. Medlock, "Optimal control for hiv treatment," *Mathematical Biosciences and Engineering*, vol. 16, no. 1, pp. 373–396, 2019.
- [13] F. A. Rihan, S. Lakshmanan, and H. Maurer, "Optimal control of tumour-immune model with time-delay and immunotherapy," *Applied Mathematics and Computation*, vol. 353, pp. 147–165, 2019.
- [14] A. Zeb, P. Kumar, V. S. Erturk, and T. Sitthiwiratham, "A new study on two different vaccinated fractional-order covid-19 models via numerical algorithms," *Journal of King Saud University Science*, vol. 34, no. 4, Article ID 101914, 2022.
- [15] K. N. Nabi, P. Kumar, and V. S. Erturk, "Projections and fractional dynamics of COVID-19 with optimal control strategies," *Chaos, Solitons & Fractals*, vol. 145, Article ID 110689, 2021.
- [16] K. N. Nabi, H. Abboubakar, and P. Kumar, "Forecasting of COVID-19 pandemic: from integer derivatives to fractional derivatives," *Chaos, Solitons & Fractals*, vol. 141, Article ID 110283, 2020.
- [17] P. Kumar, V. S. Erturk, M. Vellappandi, H. Trinh, and V. Govindaraj, "A study on the maize streak virus epidemic model by using optimized linearization-based predictor-corrector method in Caputo sense," *Chaos, Solitons & Fractals*, vol. 158, Article ID 112067, 2022.
- [18] P. Kumar, V. S. Erturk, A. Yusuf, K. S. Nisar, and S. F. Abdelwahab, "A study on canine distemper virus (cdv) and rabies epidemics in the red fox population via fractional derivatives," *Results in Physics*, vol. 25, Article ID 104281, 2021.
- [19] S. Abbas, S. Tyagi, P. Kumar, V. S. Ertürk, and S. Momani, "Stability and Bifurcation Analysis of a Fractional-Order Model of Cell-To-Cell Spread of Hiv-1 with a Discrete Time Delay," *Mathematical Methods in the Applied Sciences*, vol. 45, 2022.
- [20] N. Iqbal and Y. Karaca, "Complex fractional-order hiv diffusion model based on amplitude equations with turing patterns and turing instability," *Fractals*, vol. 29, no. 05, Article ID 2140013, 2021.
- [21] S. Hussain, E. N. Madi, N. Iqbal, T. Botmart, Y. Karaca, and W. W. Mohammed, "Fractional dynamics of vector-borne infection with sexual transmission rate and vaccination," *Mathematics*, vol. 9, no. 23, p. 3118, 2021.
- [22] F. Arif, Z. Majeed, J. U. Rahman, N. Iqbal, and J. Kafle, "Mathematical Modeling and Numerical Simulation for the Outbreak of Covid-19 Involving Loss of Immunity and Quarantined Class," *Computational and Mathematical Methods in Medicine*, vol. 2022, Article ID 3816492, 2022.
- [23] M. Salgado, S. A. Rabi, K. A. O'Connell et al., "Prolonged control of replication-competent dual-tropic human immunodeficiency virus-1 following cessation of highly active antiretroviral therapy," *Retrovirology*, vol. 8, no. 1, pp. 97–14, 2011.
- [24] W. Stöhr, S. Fidler, M. McClure et al., "Duration of hiv-1 viral suppression on cessation of antiretroviral therapy in primary infection correlates with time on therapy," *PLoS One*, vol. 8, no. 10, Article ID e78287, 2013.
- [25] O. Lambotte, F. Boufassa, Y. Madec et al., "Hiv controllers: a homogeneous group of hiv-1—infected patients with spontaneous control of viral replication," *Clinical Infectious Diseases*, vol. 41, no. 7, pp. 1053–1056, 2005.
- [26] K. A. O'Connell, J. R. Bailey, and J. N. Blankson, "Elucidating the elite: mechanisms of control in hiv-1 infection," *Trends in Pharmacological Sciences*, vol. 30, no. 12, pp. 631–637, 2009.
- [27] J. N. Blankson, "Effector mechanisms in hiv-1 infected elite controllers: highly active immune responses?" *Antiviral Research*, vol. 85, no. 1, pp. 295–302, 2010.
- [28] B. D. Walker, "Elite control of hiv infection: implications for vaccines and treatment," *Topics in HIV Medicine a publication of the International AIDS Society USA*, vol. 15, no. 4, pp. 134–136, 2007.
- [29] A. Sáez-Cirión, C. Lacabaratz, O. Lambotte et al., "Hiv controllers exhibit potent cd8 t cell capacity to suppress hiv infection ex vivo and peculiar cytotoxic t lymphocyte activation phenotype," *Proceedings of the National Academy of Sciences*, vol. 104, no. 16, pp. 6776–6781, 2007.
- [30] J. F. Okulicz, V. C. Marconi, M. L. Landrum et al., "Clinical outcomes of elite controllers, viremic controllers, and long-

- term nonprogressors in the us department of defense hiv natural history study,” *Journal of Infectious Diseases*, vol. 200, no. 11, pp. 1714–1723, 2009.
- [31] S. Grabar, H. Selinger-Leneman, S. Abgrall, G. Pialoux, L. Weiss, and D. Costagliola, “Prevalence and comparative characteristics of long-term nonprogressors and hiv controller patients in the French hospital database on hiv,” *AIDS*, vol. 23, no. 9, pp. 1163–1169, 2009.
- [32] D. D. Richman, D. M. Margolis, M. Delaney, W. C. Greene, D. Hazuda, and R. J. Pomerantz, “The challenge of finding a cure for hiv infection,” *Science*, vol. 323, no. 5919, pp. 1304–1307, 2009.
- [33] N. Chomont, M. El-Far, P. Ancuta et al., “Hiv reservoir size and persistence are driven by t cell survival and homeostatic proliferation,” *Nature Medicine*, vol. 15, no. 8, pp. 893–900, 2009.
- [34] T.-W. Chun, D. Engel, M. M. Berrey, T. Shea, L. Corey, and A. S. Fauci, “Early establishment of a pool of latently infected, resting cd4+ t cells during primary hiv-1 infection,” *Proceedings of the National Academy of Sciences*, vol. 95, no. 15, pp. 8869–8873, 1998.
- [35] J. Ananworanich, A. Schuetz, C. Vandergeeten et al., “Impact of multi-targeted antiretroviral treatment on gut t cell depletion and hiv reservoir seeding during acute hiv infection,” *PLoS One*, vol. 7, no. 3, Article ID e33948, 2012.